# Molecular characteristic analysis of single-nucleotide polymorphisms in *SLC16A9*/hMCT9

**Atsushi Yamaguchi[a, b], Yuto Mukai[b], Tomoya Sakuma[b], Yudai Suganuma[b], Ayako Furugen[b], Katsuya Narumi[b], Masaki Kobayashi[b] ***

[a]Department of Pharmacy, Hokkaido University Hospital, Kita-14-Jo, Nishi-5-Chome, Kita-ku, Sapporo, 060-8648, Japan

[b]Laboratory of Clinical Pharmaceutics & Therapeutics, Division of Pharmasciences, Faculty of Pharmaceutical Sciences, Hokkaido University, Kita-12-Jo, Nishi-6-Chome, Kita-ku, Sapporo 060-0812, Japan

[*]To whom correspondence should be addressed: Laboratory of Clinical Pharmaceutics & Therapeutics, Division of Pharmasciences, Faculty of Pharmaceutical Sciences, Hokkaido University, Kita-12-jo, Nishi-6-chome, Kita-ku, Sapporo 060-0812, Japan.
Tel/Fax: +81-11-706-3770; E-mail: masaki@pharm.hokudai.ac.jp

**Abstract**

Aims: Human monocarboxylate transporter 9 (hMCT9), encoded by *SLC16A9*, is a transporter that mediates creatine transport across the transmembrane. Previously, we reported that hMCT9 is an extracellular pH- and $Na^+$-sensitive creatine transporter with two kinetic components. Recently, some variants of hMCT9 have been found to be associated with serum uric acid levels, hyperuricemia, and gout. Among these, two single-nucleotide polymorphisms (SNPs) have also been reported: rs550527563 (L93M) and rs2242206 (T258K). However, the effect of these SNPs on hMCT9 transport activity remains unclear. This study aimed to determine the influence of hMCT9 L93M and T258K on transport characteristics.

Main methods: hMCT9 L93M and T258K were constructed by site-directed mutagenesis and expressed in *Xenopus laevis* oocyte. Transport activity of uric acid and creatine via hMCT9 were measured by using a *Xenopus laevis* oocyte heterologous expression system.

Key findings: We assessed the transport activity of uric acid and creatine and observed that hMCT9-expressing oocytes weakly transported uric acid approximately 3- to 4-fold more than water-injected oocytes. hMCT9 L93M slightly reduced the transport activity of creatine, whereas hMCT9 T258K did not affect the transport activity. Interestingly, hMCT9 T258K abolished $Na^+$ sensitivity and altered the substrate affinity from two

components to one.

Significance: In conclusion, hMCT9 SNPs affect transport activity and characteristics. hMCT9 L93M and T258K may induce dysfunction and contribute to pathologies such as hyperuricemia and gout. This is a first study to evaluate molecular characteristics of hMCT9 SNPs.

**Keywords:** *SLC16A9*; Monocarboxylate transporter 9; Uric acid; Creatine; Single-nucleotide polymorphism; *Xenopus laevis* oocyte

**Highlights**

- hMCT9 transported uric acid approximately 3–4 fold more than the negative control.
- hMCT9 L93M modestly decreases creatine transport activity.
- hMCT9 T258K abolished $Na^+$ sensitivity.
- hMCT9 T258K altered transport components and affinity for creatine.

## 1. Introduction

Human monocarboxylate transporters (hMCTs) belong to the solute carrier (SLC) 16 superfamily, consisting of 14 isoforms [1]. The topology model of hMCTs was predicted to contain 12 transmembrane domains (TMs) with intracellular C- and N-terminal domains and a large loop between TM 6 and 7 [2]. Among hMCTs, hMCT1–4 are well-characterized proton-coupled lactate transporters involved in lactate shuttling between glycolytic and oxidative cells, and astrocytes and neurons [3]. Furthermore, hMCT8 transports thyroid hormones, and its dysfunction induces the Allan–Herdon–Dudley syndrome [4]. Although most hMCTs are orphan transporters and these typical substrates are not known, they are associated with various diseases and are considered necessary in clinical practice [4].

The association between genetic variants of hMCTs and its impact on pathology and function has been reported. The most common single-nucleotide polymorphisms (SNPs) of hMCT1 (rs1049434, D490E) were found in Chinese and Japanese population [5, 6], and decreased affinity for substrates of hMCT1 [7]. In addition, it associated with overall survival and recurrence-free survivals of non-small cell lung cancer patients [8] and overall survival of colorectal cancer patients [9]. Another genetic variant of hMCT11 were associated with diabetes in Hispanic [10] and Japanese [11]. Considering these

reports, the approach from genetic variants to elucidate the function of hMCTs and diseases involved in hMCTs was valid.

Recently, genome-wide association studies (GWAS) and replication studies have revealed that hMCT9, encoded by the *SLC16A9* gene, is related to serum uric acid levels [12–20], and its SNPs are factors for hyperuricemia or gout. Huang et al. reported that a rare missense mutation in hMCT9 (rs550527563, L93M) was associated with early-onset gout [20]. Nakayama et al. investigated another common variant (rs2242206, T258K) and its SNP association with renal overload (ROL) gout [17]. In addition, Otani et al. reported that hMCT9-expressing HEK293 cells transport uric acid [21]. Previously, we constructed an hMCT9 expression system using *Xenopus laevis* oocytes and investigated its functional characteristics [22]. However, the effects of these SNPs on hMCT9 substrate transport remain unknown. We reported that hMCT9-mediated creatine transport is dependent on extracellular pH and $Na^+$ sensitivity and that the transport of creatine via hMCT9 consists of two components [22]. In this study, we constructed the hMCT9 SNP described above (hMCT9 L93M, hMCT9 T258K) and confirmed their functional characteristics compared to the hMCT9 wild-type (WT). This study aimed to elucidate the effects of hMCT9 SNPs on transport properties.

## 2. Material and methods

### *2.1. Materials and animals*

[$^{14}$C]-Uric acid was obtained from Moravek (California, USA). [$^{14}$C]-Creatine was obtained from American Radiolabeled Chemicals (St. Louis, MO, USA). Uric acid and creatine monohydrate were obtained from FUJIFILM Wako Pure Chemical Corporation (Osaka, Japan). *Xenopus laevis* frogs were obtained from Hokudo (Sapporo, Japan). The Animal Experimentation Committee of the National University Corporation, Hokkaido University (Sapporo, Japan) approved this study. All the compounds used were of the highest purity available.

### *2.2. Site-directed mutagenesis*

Site-directed mutagenesis was performed as described previously [23]. Primers containing the desired mutations are listed in Table S1. The plasmid construct was confirmed using DNA sequencing (Hokkaido System Science, Sapporo, Japan).

### *2.3. Complementary RNA (cRNA) expression in X. laevis oocytes*

hMCT9 WT, L93M, and T258K were expressed in oocytes, as described previously [22]. The AmpliCap-Max T7 High-Yield Message Maker Kit (CELLSCRIPT,

Madison, WI, USA) was used for *in vitro* cRNA synthesis. *X. laevis* oocytes were injected with 50 ng of cRNA encoding hMCT9 WT, L93M, and T258K; water was used as a negative control.

### *2.4. Immunohistochemistry*

Immunohistochemical analysis was performed as described previously [22]. Oocytes were stained with rabbit anti-hMCT9 antibody (ab184870; Abcam, Cambridge, UK), which recognizes intracellular loop 3. The prepared oocytes were monitored under an FV10i confocal laser scanning microscope (Olympus Corporation, Tokyo, Japan).

### *2.5. Transmembrane domain prediction*

The putative transmembrane domains of hMCT9 were predicted using the Constrained Consensus TOPology (CCTOP) prediction web server (http://cctop.enzim.ttk.mta.hu/) [24], and the predicted 2D topology model was visualized using the PROTTER web application (http://wlab.ethz.ch/protter/start/) [25].

### *2.6. Uric acid and creatine transport assay*

The transport activity of hMCT9 was assessed according to our previously

described method [22], with some modifications. Briefly, after equilibration for 10 min at 25 °C in a standard buffer, three to five oocytes were incubated for 60 min at 25 °C in a standard buffer containing 5 μM [$^{14}$C]-uric acid or 10 μM [$^{14}$C]-creatine. We conducted an uptake assay under specific conditions to elucidate the molecular characteristics. For pH sensitivity, we used a standard buffer at various pH values. For $Na^+$ sensitivity, we used a standard buffer containing 100 mM NaCl or choline chloride. MES was used as a buffer at pH 5.5–6.5, and HEPES was used as a buffer at pH 7.4–7.5. The specific uptake was calculated by subtracting the uptake in water-injected oocytes from that in cRNA-injected oocytes.

*2.7. Data analysis*

All data were analyzed using SigmaPlot 14.5 (Systat Software, San Jose, CA, USA). Data were fitted to the Michaelis–Menten equation with single or two saturable components, and Km values were estimated using the Eadie–Hofstee plot:

$$V = V_{max} \cdot S/(K_m + S) \text{ or } V = V_{max1} \cdot S/(K_{m,\,high} + S) + V_{max2} \cdot S/(K_{m,\,low} + S)$$

where V is the uptake rate, S is the creatine concentration, and Km is the Michaelis constant.

*2.8. Statistical analysis*

Statistical analyses were performed using the Tukey-Kramer tests. Data were analyzed using SigmaPlot 14.5, and differences were considered statistically significant at $p < 0.05$.

## 3. Results

*3.1. Evaluation of hMCT9-mediated uric acid and creatine*

First, we predicted the transmembrane domains of hMCT9, which contain 12 TMs (Fig. S1). Based on this prediction, we confirmed the positions of L93 and T258. hMCT9 L93 was embedded in TM3, and hMCT9 T258 was situated in a large intracellular loop. Next, we induced mutagenesis in hMCT9 L93M and T258K, and expressed them in *Xenopus laevis* oocytes. Immunohistochemical staining revealed that hMCT9 WT, L93M, and T258K were expressed in oocytes and were adequately localized to the oocyte membrane (Fig. 1). We investigated the uric acid transport activity of hMCT9 because hMCT9 and its SNPs are involved in serum uric acid levels. Oocytes-expressed hMCT9 WT weakly transport uric acid, approximately 3- to 4-fold more than water-injected oocytes, with statistical significance (Fig. 2A). Furthermore, high

concentrations of uric acid (1 mM) did not inhibit the transport activity of hMCT9 WT (Fig. 2B). We then evaluated the effects of SNPs, hMCT9 L93M and T258K, on the creatine transport of hMCT9 because of the high transport activity of creatine [26]. hMCT9 L93M slightly attenuated transport activity while there is no significant difference. hMCT9 T258K transported creatine, similar to hMCT9 WT (Fig. 2B).

*3.2. Influence of extracellular pH and $Na^+$ composition on hMCT9 SNPs*

To evaluate the molecular effects of hMCT9 L93M and T258K on creatine transport in more detail, we next conducted an uptake study with a pH gradient because hMCT9 was sensitive to $H^+$ gradient changes and the transport activity of hMCT9 increases as the extracellular pH increases [22]. Similar to hMCT9 WT, hMCT9 L93M and T258K transported creatine with an increase in extracellular pH (Fig. 3A), indicating that L93 and T258 were not involved in pH sensitivity with statistical significance in hMCT9 WT and T258K at pH 7.5 compared at pH 5.5, respectively, and even though without statistical significance in hMCT9 L93M at pH 7.5 compared at pH 5.5. Regarding $Na^+$ sensitivity, the transport activity of hMCT9 WT decreased approximately by half in the absence of $Na^+$, with statistical significance, as reported in a previous study [22]. hMCT9 L93M decreased to the same degree as hMCT9 WT while there was no statistical

significance (Fig. 3B). hMCT9 T258K transported creatine almost equally (no statistical significance), regardless of the presence of $Na^+$ ions (Fig. 3B).

*3.3. Kinetic analysis of hMCT9 SNPs mediated creatine transport*

Finally, we evaluated the affinity of hMCT9 WT, L93M, and T258K for creatine. hMCT9 WT transported creatine at high substrate concentration with saturation (Fig. 4A) [22], and Eadie–Hofstee plot indicated the presence of two components with Km and Vmax values of 16.49 ± 1.35 mM and 83.3 ± 5.32 fmol/min/oocyte for high affinity and of 130.08 ± 25.45 mM and 414.0 ± 60.17 fmol/min/oocyte for low affinity, respectively (Fig. 4B). hMCT9 L93M also had two components according to Eadie–Hofstee plot with the Km and Vmax values of 15.26 ± 2.01 mM and 68.3 ± 6.91 fmol/min/oocyte for high affinity and of 146.73 ± 33.51 and 391.6 ± 68.14 fmol/min/oocyte for low affinity, respectively (Fig. 4C and 4D). Compared to hMCT9 WT and L93M, hMCT9 T258K also showed a saturation (Fig. 4E) but a linear in Eadie–Hofstee plots (Fig. 4F). The Km and Vmax values of hMCT9 T258K were estimated to be 55.66 ± 6.58 mM and 210.77 ± 19.12 fmol/min/oocyte, respectively (Fig. 4F), which were intermediate between high and low-affinity Km and Vmax values of hMCT9 WT. The regression values of the Michaelis–Menten equation and Eadie–Hofstee plot are described in Table S2. hMCT9 WT, L93M, and T258K fitted well the Michaelis–Menten equation in one- and two-

component models. However, the regression values of hMCT9 WT and hMCT9 L93M in the Eadie–Hofstee plot improved in the two- compared to the one-component model, while hMCT9 T258K had similar values in both one and two components.

## 4. Discussion

In this study, we performed a functional analysis of two SNPs of hMCT9 that are associated with gout and are involved in hMCT9 transport characteristics. First, we examined the ability of hMCT9 to transport uric acid because certain genetic variants of hMCT9 have been reported to affect the plasma concentrations of uric acid, hyperuricemia, and gout [12–20]. Although oocytes expressing hMCT9 transport uric acid as well as previously reported hMCT9 expressing HEK293 cell line [21], the transport activity of uric acid via hMCT9 was approximately 3- to 4-fold more than water-injected oocytes (Fig. 2A). In addition, a high concentration of uric acid (1 mM) did not affect hMCT9 WT. Previously, we described that excessive creatine (10 mM) inhibited creatine transport by approximately 40%. This competitive substrate concentration was lower than that of high- and low-affinity Km values of hMCT9 WT (16.49 ± 1.35 mM and 130.08 ± 25.45 mM, respectively). Consequently, uric acid (1 mM) did not inhibit hMCT9 creatine transport due to the high capacity of hMCT9 WT for substrate transport. Further experimental data are needed to evaluate molecular characteristics of hMCT9 for uric acid transport.

As for uric acid transporters, a large GWAS study with 28,141 individuals of European descent revealed that *SLC2A9, ABCG2, SLC17A1,* and *SLC22A12* were

strongly associated with serum uric acid levels compared with *SLC16A9*/MCT9 [14]. In another study, the knockout of aldehyde dehydrogenase *(aldh) 16A1* in mice upregulated *abcc4* and *slc16a9* and downregulated *slc17a3*, associated with serum uric acid levels [27]. These reports suggest that transporters may cooperatively regulate serum uric acid levels. For example, sodium-coupled monocarboxylate transporter (SMCT) 1 *(SLC5A8)* and SMCT2 *(SLC5A12)* transport lactate and nicotinate, and form complexes with PDZK1 and URAT1 *(SLC22A12)* [28]. Because URAT1 is an exchanger of uric acid and anions, SMCTs are important for its function [29].

Furthermore, a meta-analysis of GWAS reported that rs12356193 within *SLC16A9* was associated with DL-carnitine and propionyl-L-carnitine concentrations as well as serum uric acid levels [14]. In addition, Suhre et al. reported that hMCT9 is a carnitine efflux transporter [30]. Consequently, we hypothesized that hMCT9 may indirectly affect uric acid levels via creatine transport, and we evaluated the effect of hMCT9 SNPs on functional creatine transport, as the relationship between creatine or transport and serum uric acid levels is not well known. Further studies are required to elucidate the molecular mechanisms of these physiological conditions.

hMCT9 L93M was adequately expressed in the oocyte membrane (Fig. 1B). However, its creatine transport activity was slightly attenuated (Fig. 2B) compared with

hMCT9 WT, without alteration of other characteristics, such as pH, $Na^+$ sensitivity (Fig. 3), and substrate affinity (Fig. 4). Since hMCT9 L93 was embedded in TM3 (Fig. S1), hMCT9 L93 might be positioned towards the extracellular side in an outward open conformation and be involved in the creatine transport pathway, but not in a substrate-binding site. hMCT9 is expressed ubiquitously, especially in the kidney [2], and its expression in the apical membrane of the proximal convoluted tubule of the kidney influences uric acid homeostasis [31]. Although the clinical implications of hMCT9 L93M are not clear, its functional reduction may influence serum uric acid levels, inducing early onset gout [20].

hMCT9 T258K was expressed in oocytes (Fig. 1C), and transport activity and creatine pH sensitivity were similar to those of hMCT9 WT (Fig. 2B and 3A). The creatine transport activity of hMCT9 T258K was retained regardless of the presence of $Na^+$ ions (Fig. 3B), indicating that hMCT9 T258 was associated with $Na^+$ sensitivity. Threonine is a hydrophilic amino acid with a hydroxyl group interacting with $Na^+$ ions. The T453 residue of *SLC38A9*, which belongs to the SLC family as hMCT9, recognizes $Na^+$ [32]. The sodium-dependent betaine symporter BetP has two $Na^+$-binding sites: T467 for the Na1 site and T246 and T250 for the Na2 site [33]. Therefore, it is appropriate for hMCT9 T258 to exhibit $Na^+$ sensitivity. According to the kinetic analysis of hMCT9

T258K, hMCT9 T258K showed saturation (Fig. 4E) but a linear in Eadie–Hofstee plots (Fig. 4F) compared to hMCT9 WT, and its Km and Vmax values were intermediate between the high- and low-affinity Km and Vmax values of hMCT9 WT. These results indicated that hMCT9 T258 intracellular large loop affects substrate affinity, which agrees with hMCT1 and hMCT4. The large intracellular loops of hMCT1 and hMCT4 are involved in the affinity for lactate, a typical substrate of hMCT1 and hMCT4 [34]. Similar to hMCT9 WT, certain transporters have two components, such as OATPs [22, 23]. Accordingly, two hypotheses have been proposed: (1) hMCT9 has two substrate-binding sites with different affinities; (2) hMCT9 has two kinetically discernible conformations at low and high concentrations. When hMCT9 has two transport pathways with different substrate-binding sites, hMCT9 T258 could be involved in the $Na^+$-sensitive pathway, and hMCT9 T258K abolishes $Na^+$ sensitivity and reduces the number of affinity sites. It may be reasonable that hMCT9 WT transports creatine even without $Na^+$ (Fig. 3B). However, the Km value of hMCT9 T258K was not similar to that of hMCT9 WT. In one case, we considered that hMCT9 T258K might lose high or low affinity, whereas the other site alters the affinity. In other possibility, we propose that $Na^+$ ions allow hMCT9 to adopt two conformations with different affinities. In other words, abolishing $Na^+$ sensitivity in hMCT9 T258K contributed to conformational changes, enabling hMCT9

T258K to affect the affinity of the two components to one. Although the molecular mechanism underlying the affinity conversion from the two components to one in hMCT9 T258K is controversial, hMCT9 T258K may be involved in pathologies such as hyperuricemia and gout caused by physiological dysfunction. In a clinical study, hMCT9 T258K increased the risk of ROL gout and not renal under-excretion gout [17], indicating that hMCT9 is involved in intestinal uric acid excretion. The uric acid transporter ABCG2 contributes to the excretion of uric acid in the gut and decreases serum uric acid decrease [33, 34]. In this study, hMCT9 T258K maintained its transport activity; however, the molecular functions of $Na^+$ sensitivity and substrate affinity were altered. These alterations could induce dysfunction in the intestine and not in the kidneys because the concentrations of $Na^+$ and substrate could vary between these tissues, which may explain why hMCT9 T258K induced ROL gout.

## Conclusion

In conclusion, we functionally evaluated the hMCT9 SNPs, hMCT9 L93M and T258K, for the first time, revealing that hMCT9 L93M weakly decreased transport activity and that hMCT9 T258K lost $Na^+$ sensitivity and altered substrate affinity. These results contribute to the elucidation of the transport mechanism of hMCT9 and the pathology

associated with hMCT9 SNPs.

## Author contributions

AY and MK designed the experiments. AY wrote the first draft of the manuscript. AY and YM conducted experiments. AY, YM, and MK analyzed the results. All the authors contributed to writing manuscript, reviewed the results and approved the final version of the manuscript.

## Conflict of interest

The authors have no conflicts of interest to declare.

## Acknowledgments

This work was supported by a grant from the Japan Society for the Promotion of Science (JSPS) KAKENHI (Grant number: 22H04330, provided to AY).

We would like to thank Editage (http://www.editage.jp) for the English language editing.

We would like to thank the Open Facility, Global Facility Center, Creative Research Institution, and Hokkaido University for allowing us to conduct immunohistochemistry analysis using an FV10i confocal laser scanning microscope and for providing insight

and expertise that greatly assisted the research.

## References

[1] A.P. Halestrap, M.C. Wilson, The monocarboxylate transporter family-role and regulation, IUBMB Life. 64 (2012) 109–119. https://doi.org/10.1002/iub.572.

[2] A.P. Halestrap, The SLC16 gene family - structure, role and regulation in health and disease, Mol. Aspects Med. 34 (2013) 337–349. https://doi.org/10.1016/j.mam.2012.05.003.

[3] M. Kobayashi, K. Narumi, A. Furugen, K. Iseki, Transport function, regulation, and biology of human monocarboxylate transporter 1 (hMCT1) and 4 (hMCT4), Pharmacol. Ther. 226 (2021) 107862. https://doi.org/10.1016/j.pharmthera.2021.107862.

[4] P. Fisel, E. Schaeffeler, M. Schwab, Clinical and Functional Relevance of the Monocarboxylate Transporter Family in Disease Pathophysiology and Drug Therapy, Clin. Transl. Sci. 11 (2018) 352–364. https://doi.org/10.1111/cts.12551.

[5] C.B. Lean, E.J.D. Lee, Genetic variations in the MCT1 (SLC16A1) gene in the Chinese population of Singapore., Drug Metab. Pharmacokinet. 24 (2009) 469–474. https://doi.org/10.2133/dmpk.24.469.

[6] Y. Kimura, M. Kobayashi, M. Asari, I. Higuchi, K. Narumi, A. Furugen, K. Iseki, Genetic variations in the monocarboxylate transporter genes (SLC16A1,

SLC16A3, and SLC16A11) in the Japanese population., Drug Metab. Pharmacokinet. 33 (2018) 215–218. https://doi.org/10.1016/j.dmpk.2018.05.001.

[7] S. Sasaki, Y. Futagi, M. Kobayashi, J. Ogura, K. Iseki, Functional characterization of 5-oxoproline transport via SLC16A1/MCT1., J. Biol. Chem. 290 (2015) 2303–2311. https://doi.org/10.1074/jbc.M114.581892.

[8] X. Guo, C. Chen, B. Liu, Y. Wu, Y. Chen, X. Zhou, X. Huang, X. Li, H. Yang, Z. Chen, J. Xing, Genetic variations in monocarboxylate transporter genes as predictors of clinical outcomes in non-small cell lung cancer., Tumour Biol. J. Int. Soc. Oncodevelopmental Biol. Med. 36 (2015) 3931–3939. https://doi.org/10.1007/s13277-014-3036-0.

[9] F. Fei, X. Guo, Y. Chen, X. Liu, J. Tu, J. Xing, Z. Chen, J. Ji, X. He, Polymorphisms of monocarboxylate transporter genes are associated with clinical outcomes in patients with colorectal cancer., J. Cancer Res. Clin. Oncol. 141 (2015) 1095–1102. https://doi.org/10.1007/s00432-014-1877-y.

[10] B.A. Hidalgo, T. Sofer, Q. Qi, N. Schneiderman, Y.-D.I. Chen, R.C. Kaplan, M.L. Avilés-Santa, K.E. North, D.K. Arnett, A. Szpiro, J. Cai, B. Yu, E. Boerwinkle, G. Papanicolaou, C.C. Laurie, J.I. Rotter, A.M. Stilp, Associations between SLC16A11 variants and diabetes in the Hispanic Community Health

Study/Study of Latinos (HCHS/SOL)., Sci. Rep. 9 (2019) 843. https://doi.org/10.1038/s41598-018-35707-7.

[11] Y. Kimura, I. Higuchi, M. Kobayashi, A. Furugen, K. Narumi, Y. Suzuki, H. Miyoshi, A. Nakamura, T. Atsumi, K. Iseki, The association between SLC16A11 haplotype and lipid metabolism in Japanese patients with type 2 diabetes., Drug Metab. Pharmacokinet. 37 (2021) 100376. https://doi.org/10.1016/j.dmpk.2020.100376.

[12] K. Stark, W. Reinhard, M. Grassl, J. Erdmann, H. Schunkert, T. Illig, C. Hengstenberg, Common polymorphisms influencing serum uric acid levels contribute to susceptibility to gout, but not to coronary artery disease, PLoS One. 4 (2009) e7729. https://doi.org/10.1371/journal.pone.0007729.

[13] P. van der Harst, S.J.L. Bakker, R.A. de Boer, B.H.R. Wolffenbuttel, T. Johnson, M.J. Caulfield, G. Navis, Replication of the five novel loci for uric acid concentrations and potential mediating mechanisms, Hum. Mol. Genet. 19 (2009) 387–395. https://doi.org/10.1093/hmg/ddp489.

[14] M. Kolz, T. Johnson, S. Sanna, A. Teumer, V. Vitart, M. Perola, M. Mangino, E. Albrecht, C. Wallace, M. Farrall, A. Johansson, D.R. Nyholt, Y. Aulchenko, J.S. Beckmann, S. Bergmann, M. Bochud, M. Brown, H. Campbell, J. Connell, A.

Dominiczak, G. Homuth, C. Lamina, M.I. McCarthy, T. Meitinger, V. Mooser, P. Munroe, M. Nauck, J. Peden, H. Prokisch, P. Salo, V. Salomaa, N.J. Samani, D. Schlessinger, M. Uda, U. Völker, G. Waeber, D. Waterworth, R. Wang Sattler, A.F. Wright, J. Adamski, J.B. Whitfield, U. Gyllensten, J.F. Wilson, I. Rudan, P. Pramstaller, H. Watkins, A. Doering, H.E. Wichmann, T.D. Spector, L. Peltonen, H. Völzke, R. Nagaraja, P. Vollenweider, M. Caulfield, T. Illig, C. Gieger, Meta-analysis of 28,141 individuals identifies common variants within five new loci that influence uric acid concentrations, PLoS Genet. 5 (2009) e1000504. https://doi.org/10.1371/journal.pgen.1000504.

[15] G. Gunjaca, M. Boban, M. Pehlić, T. Zemunik, D. Budimir, I. Kolcić, G. Lauc, I. Rudan, O. Polasek, Predictive value of 8 genetic loci for serum uric acid concentration, Croat. Med. J. 51 (2010) 23–31. https://doi.org/10.3325/cmj.2010.51.23.

[16] Y.H. Lee, G.G. Song, Pathway analysis of genome-wide association studies on uric acid concentrations, Hum. Immunol. 73 (2012) 805–810. https://doi.org/10.1016/j.humimm.2012.05.004.

[17] A. Nakayama, H. Matsuo, T. Shimizu, H. Ogata, Y. Takada, H. Nakashima, T. Nakamura, S. Shimizu, T. Chiba, M. Sakiyama, C. Ushiyama, T. Takada, K.

Inoue, S. Kawai, A. Hishida, K. Wakai, N. Hamajima, K. Ichida, Y. Sakurai, Y. Kato, T. Shimizu, N. Shinomiya, Common missense variant of monocarboxylate transporter 9 (MCT9/SLC16A9) gene is associated with renal overload gout, but not with all gout susceptibility, Hum. Cell. 26 (2013) 133–136. https://doi.org/10.1007/s13577-013-0073-8.

[18] W. Wan, X. Xu, D.B. Zhao, Y.F. Pang, Y.X. Wang, Polymorphisms of uric transporter proteins in the pathogenesis of gout in a Chinese Han population, Genet. Mol. Res. 14 (2015) 2546–2550. https://doi.org/10.4238/2015.March.30.13.

[19] A. Alghubayshi, A. Edelman, K. Alrajeh, Y. Roman, Genetic assessment of hyperuricemia and gout in Asian, Native Hawaiian, and Pacific Islander subgroups of pregnant women: biospecimens repository cross-sectional study, BMC Rheumatol. 6 (2022) 1. https://doi.org/10.1186/s41927-021-00239-7.

[20] X.F. Huang, L. Sun, C. Zhang, Z. Zhou, H. Chen, L. Zhang, M.A. Brown, X. Xia, Whole-Exome Sequencing Reveals a Rare Missense Variant in SLC16A9 in a Pedigree with Early-Onset Gout, Biomed Res. Int. 2020 (2020) 4321419. https://doi.org/10.1155/2020/4321419.

[21] N. Otani, Y. Kurata, N. Maharani, M. Kuwabara, N. Ikeda, T. Notsu, P. Li, J.

Miake, A. Yoshida, H. Sakaguchi, K. Higaki, N. Nakasone, M. Tsuneto, Y. Shirayoshi, M. Ouchi, H. Ninomiya, K. Yamamoto, N. Anzai, I. Hisatome, Evidence for Urate Uptake Through Monocarboxylate Transporter 9 Expressed in Mammalian Cells and Its Enhancement by Heat Shock., Circ. Reports. 2 (2020) 425–432. https://doi.org/10.1253/circrep.CR-20-0016.

[22] Y. Futagi, K. Narumi, A. Furugen, M. Kobayashi, K. Iseki, Molecular characterization of the orphan transporter SLC16A9, an extracellular pH- and Na+-sensitive creatine transporter, Biochem. Biophys. Res. Commun. 522 (2020) 539–544. https://doi.org/10.1016/j.bbrc.2019.11.137.

[23] A. Yamaguchi, Y. Futagi, M. Kobayashi, K. Narumi, A. Furugen, K. Iseki, Extracellular lysine 38 plays a crucial role in pH-dependent transport via human monocarboxylate transporter 1, Biochim. Biophys. Acta Biomembr. 1862 (2020) 183068. https://doi.org/10.1016/j.bbamem.2019.183068.

[24] L. Dobson, I. Reményi, G.E. Tusnády, CCTOP: a Consensus Constrained TOPology prediction web server, Nucleic Acids Res. 43 (2015) W408–W412. https://doi.org/10.1093/nar/gkv451.

[25] U. Omasits, C.H. Ahrens, S. Müller, B. Wollscheid, Protter: interactive protein feature visualization and integration with experimental proteomic data,

Bioinformatics. 30 (2014) 884–886.
https://doi.org/10.1093/bioinformatics/btt607.

[26] Y. Futagi, K. Narumi, A. Furugen, M. Kobayashi, K. Iseki, Molecular characterization of the orphan transporter SLC16A9, an extracellular pH- and Na(+)-sensitive creatine transporter, Biochem. Biophys. Res. Commun. 522 (2020) 539–544. https://doi.org/10.1016/j.bbrc.2019.11.137.

[27] M.P. Leask, T.R. Merriman, The genetic basis of urate control and gout: Insights into molecular pathogenesis from follow-up study of genome-wide association study loci., Best Pract. Res. Clin. Rheumatol. 35 (2021) 101721. https://doi.org/10.1016/j.berh.2021.101721.

[28] S. Srivastava, K. Nakagawa, X. He, T. Kimura, T. Fukutomi, S. Miyauchi, H. Sakurai, N. Anzai, Identification of the multivalent PDZ protein PDZK1 as a binding partner of sodium-coupled monocarboxylate transporter SMCT1 (SLC5A8) and SMCT2 (SLC5A12)., J. Physiol. Sci. 69 (2019) 399–408. https://doi.org/10.1007/s12576-018-00658-1.

[29] N. Anzai, Y. Kanai, H. Endou, New insights into renal transport of urate., Curr. Opin. Rheumatol. 19 (2007) 151–157. https://doi.org/10.1097/BOR.0b013e328032781a.

[30] K. Suhre, S.-Y. Shin, A.-K. Petersen, R.P. Mohney, D. Meredith, B. Wägele, E. Altmaier, P. Deloukas, J. Erdmann, E. Grundberg, C.J. Hammond, M.H. de Angelis, G. Kastenmüller, A. Köttgen, F. Kronenberg, M. Mangino, C. Meisinger, T. Meitinger, H.-W. Mewes, M. V Milburn, C. Prehn, J. Raffler, J.S. Ried, W. Römisch-Margl, N.J. Samani, K.S. Small, H.-E. Wichmann, G. Zhai, T. Illig, T.D. Spector, J. Adamski, N. Soranzo, C. Gieger, Human metabolic individuality in biomedical and pharmaceutical research., Nature. 477 (2011) 54–60. https://doi.org/10.1038/nature10354.

[31] G. Charkoftaki, Y. Chen, M. Han, M. Sandoval, X. Yu, H. Zhao, D.J. Orlicky, D.C. Thompson, V. Vasiliou, Transcriptomic analysis and plasma metabolomics in Aldh16a1-null mice reveals a potential role of ALDH16A1 in renal function., Chem. Biol. Interact. 276 (2017) 15–22. https://doi.org/10.1016/j.cbi.2017.02.013.

[32] M. Scalise, M. Galluccio, L. Pochini, J. Cosco, M. Trotta, M. Rebsamen, G. Superti-Furga, C. Indiveri, Insights into the transport side of the human SLC38A9 transceptor, Biochim. Biophys. Acta Biomembr. 1861 (2019) 1558–1567. https://doi.org/10.1016/j.bbamem.2019.07.006.

[33] K. Khafizov, C. Perez, C. Koshy, M. Quick, K. Fendler, C. Ziegler, L.R. Forrest,

Investigation of the sodium-binding sites in the sodium-coupled betaine transporter BetP, Proc. Natl. Acad. Sci. U. S. A. 109 (2012) E3035–E3044. https://doi.org/10.1073/pnas.1209039109.

[34] Y. Futagi, S. Sasaki, M. Kobayashi, K. Narumi, A. Furugen, K. Iseki, The flexible cytoplasmic loop 3 contributes to the substrate affinity of human monocarboxylate transporters, Biochim. Biophys. Acta Biomembr. 1859 (2017) 1790–1795. https://doi.org/10.1016/j.bbamem.2017.05.014.

[35] A. Bodo, E. Bakos, F. Szeri, A. Varadi, B. Sarkadi, Differential modulation of the human liver conjugate transporters MRP2 and MRP3 by bile acids and organic anions, J. Biol. Chem. 278 (2003) 23529–23537. https://doi.org/10.1074/jbc.M303515200.

[36] I. Tamai, T. Nozawa, M. Koshida, J. Nezu, Y. Sai, A. Tsuji, Functional characterization of human organic anion transporting polypeptide B (OATP-B) in comparison with liver-specific OATP-C, Pharm. Res. 18 (2001) 1262–1269. https://doi.org/10.1023/a:1013077609227.

[37] H. Yin, N. Liu, J. Chen, The Role of the Intestine in the Development of Hyperuricemia., Front. Immunol. 13 (2022) 845684. https://doi.org/10.3389/fimmu.2022.845684.

[38] T. Zhao, L. Cao, C. Lin, R. Xu, X. Du, M. Zhou, X. Yang, W. Wan, H. Zou, X. Zhu, Intestinal uric acid excretion contributes to serum uric acid decrease during acute gout attack., Rheumatology (Oxford). kead139 (2023) Online ahead of print. https://doi.org/10.1093/rheumatology/kead139.

**Figure legends**

Fig. 1. Immunofluorescence staining of hMCT9 SNPs.

Expression of hMCT9 WT (A), L93M (B), and T258K (C), and water-injected oocytes (D) used as negative controls. The oocyte membranes were examined by fluorescence microscopy using an anti-hMCT9 antibody.

Fig. 2. Transport activity of uric acid and creatin via hMCT9 SNPs.

Uptake of [$^{14}$C]-uric acid (5 μM) was measured in oocytes expressing indicated hMCT9 WT, L93M, and T258K, and in water-injected oocytes for 60 min at 25 °C with pH 7.4 (A). Transport activity of [$^{14}$C]-creatine was monitored for 60 min incubation with 10 μM creatine with or without 1 mM uric acid at 25 °C with pH 7.4 (B), and specific uptake was calculated by subtracting the uptake in water-injected oocytes from that in cRNA-injected oocytes. All data are the mean values with S.E. from three independent experiments, each performed with three to five technical replicates. *, $p < 0.05$, compared water using the Tukey-Kramer test.

Fig. 3. Effects of extracellular pH and $Na^+$ ion on hMCT9 SNPs.

pH sensitivity assessed after incubation with 10 μM [$^{14}$C]-creatine with various pH values

for 60 min at 25 °C (A). To evaluate the effects of $Na^+$ ion, [$^{14}$C]-creatine uptake was measured for 60 min at 25 °C with pH 7.4 using a standard buffer containing 100 mM NaCl or choline chloride (B). The specific uptake was calculated by subtracting the uptake in water-injected oocytes from that in cRNA-injected oocytes. All data are the mean values with S.E. from three independent experiments, each performed with three to five technical replicates. [a], $p < 0.05$, compared with WT at pH 5.5, [b], $p < 0.05$, compared with T258K at pH 5.5, and [c], $p < 0.05$, compared with WT $Na^+$ (-) using the Tukey-Kramer test.

Fig. 4. The kinetic analysis of hMCT9 SNPs.

The concentration dependence of [$^{14}$C]-creatine uptake via hMCT9 was assayed at various substrate concentrations in hMCT9 WT (A), hMCT9 L93M (C), and hMCT9 T258K (E) for 60 min at 25 °C with pH 7.4. The data were fitted to the Michaelis-Menten equation for two saturable components (A and C) and a single saturable component (E). Eadie–Hofstee plot of the data, in which the creatine uptake rate (V) is plotted against V/[creatine] (V/S) (B, D, F). The specific uptake was calculated by subtracting the uptake in water-injected oocytes from that in cRNA-injected oocytes. All data are the mean values with S.E. from four independent experiments, each performed with three to five

technical replicates.

Fig. S1. hMCT9 2D topology model.

Transmembrane domains were predicted using the CCTOP web server and described using the PROTTER web application. The residues positioned at L93 and T258 are highlighted in green and blue, respectively.

1 Fig.1

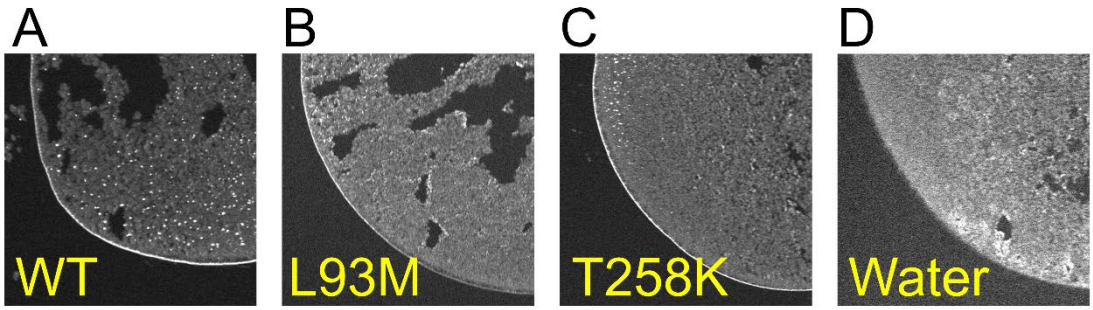


2

1 Fig.2

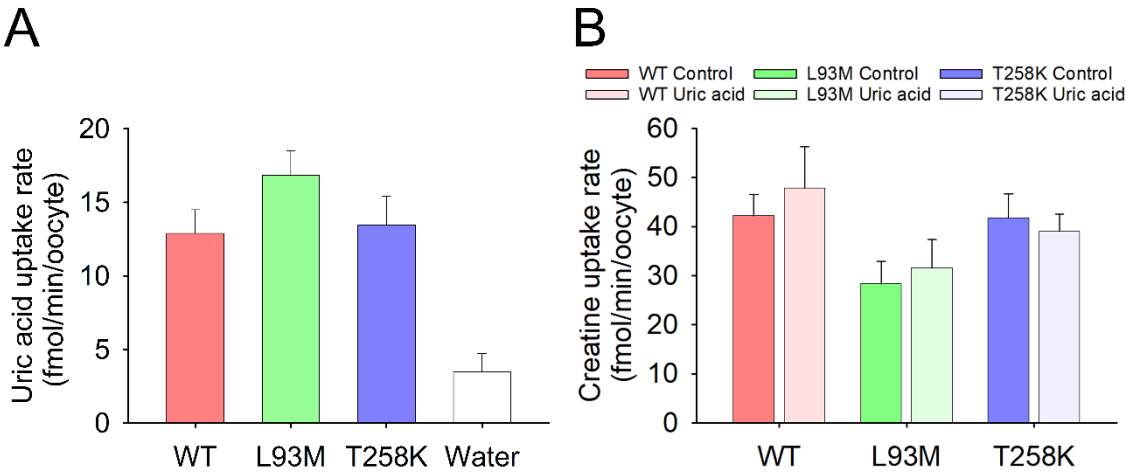
A
Uric acid uptake rate (fmol/min/oocyte)
20
15
10
5
0
WT
L93M
T258K
Water
B
WT Control
L93M Control
T258K Control
WT Uric acid
L93M Uric acid
T258K Uric acid
Creatine uptake rate (fmol/min/oocyte)
60
50
40
30
20
10
0
WT
L93M
T258K

2

1 Fig.3

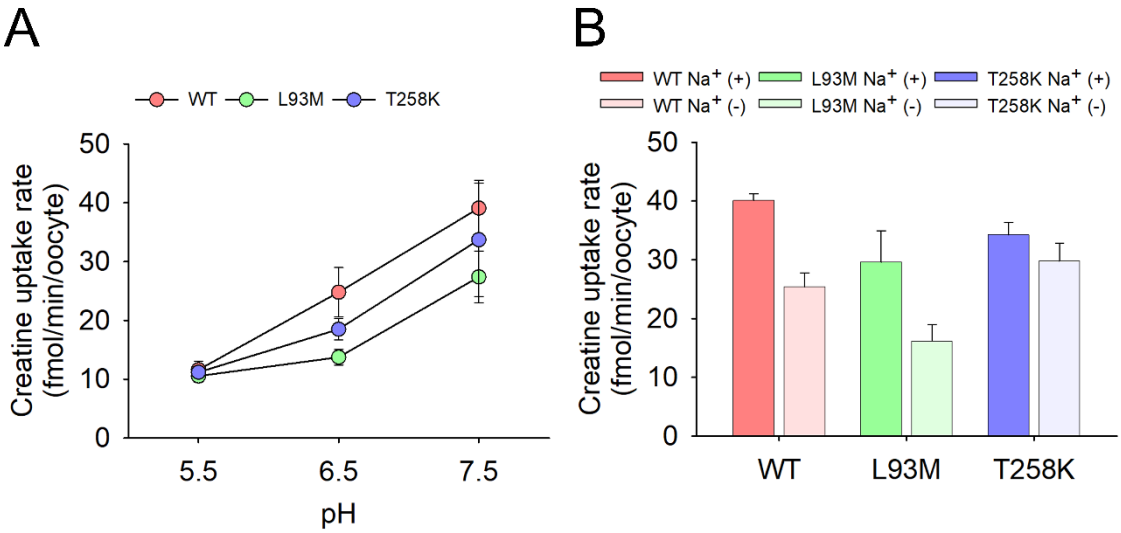
A
WT
L93M
T258K
Creatine uptake rate
(fmol/min/oocyte)
50
40
30
20
10
0
5.5
6.5
7.5
pH
B
WT Na+ (+)
L93M Na+ (+)
T258K Na+ (+)
WT Na+ (-)
L93M Na+ (-)
T258K Na+ (-)
Creatine uptake rate
(fmol/min/oocyte)
50
40
30
20
10
0
WT
L93M
T258K

2

1 Fig.4

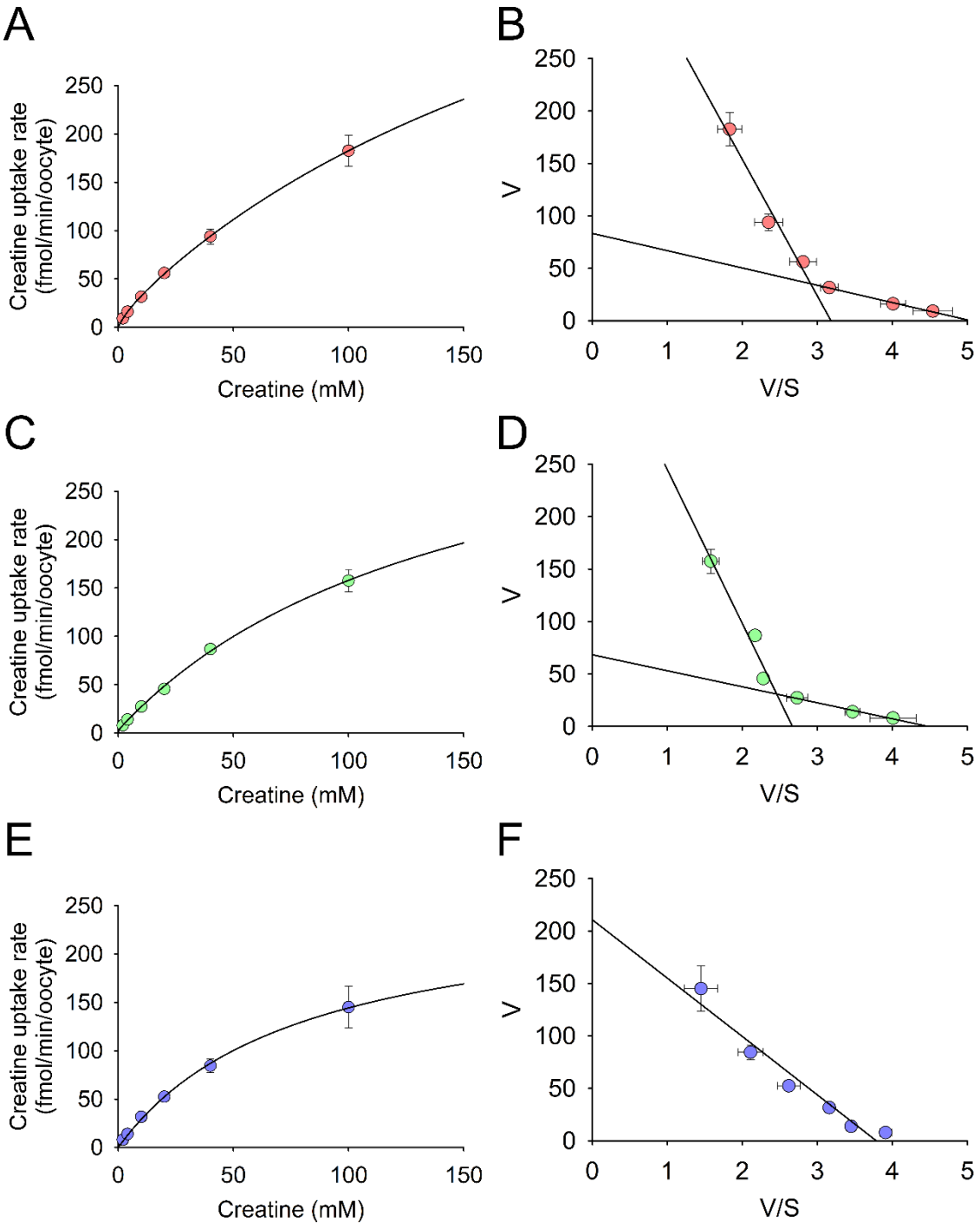
A
B
C
D
E
F
Creatine uptake rate (fmol/min/oocyte)
Creatine (mM)
V
V/S
0
50
100
150
200
250
1
2
3
4
5

2